Lattice Boltzmann method for 2D flows in curvilinear coordinates

Ljubomir Budinski

ABSTRACT

In order to improve efficiency and accuracy, while maintaining an ease of modeling flows with the lattice Boltzmann approach in domains having complex geometry, a method for modeling equations of 2D flow in curvilinear coordinates has been developed. Both the transformed shallow water equations and the transformed 2D Navier-Stokes equations in the horizontal plane were synchronized with the equilibrium distribution function and the force term in the rectangular lattice. Since the solution of these equations takes place in the classical rectangular lattice environment, boundary conditions are modeled in the standard form of already existing simple methods (bounce-back), not requiring any additional functions. Owing to this and to the fact that the proposed method ensures a more accurate fitting of equations, even to domains of interest having complex geometry, the accuracy of solution is significantly increased, while the simplicity of the standard lattice Boltzmann approach is maintained. For the shallow water equations transformed in curvilinear coordinates, the proposed procedure is verified in three different hydraulic problems, all characterized by complex geometry.

Key words | 2D flow equations, complex geometry, curvilinear coordinates, lattice Boltzmann method

Ljubomir Budinski
Faculty of Civil Engineering Subotica,
University of Novi Sad,
Kozaračka 2a,
24000 Subotica,
Serbia
E-mail: *ljubab@open.telekom.rs*;
ljubab@gf.uns.ac.rs

INTRODUCTION

Since McNamara & Zanetti (1988) eliminated the Bolean structure of the Lattice Gas Automata (LGA) by introducing the lattice Boltzmann method (LBM) two decades ago, this method has evolved into a powerful concept suitable for modeling very complex and demanding hydraulic problems. Based on kinetic theory, in which fluid is defined as a discretized phase-space system made of individual particles colliding with each other while advancing with pre-defined velocities along their trajectories, it has allowed the establishment of a numerical procedure of parallel nature characterized by high accuracy, efficiency and simplicity in implementing the elements of the model. As such it is present in up-to-date flow studies both in the field of science and engineering.

As the aim of numerical modeling is to describe and learn relevant physical processes controlled by actual natural conditions, a demand for describing and modeling flow in domains of arbitrary geometry arose even in the early days of the LGA models, such as square lattice model HPP (Hardy-Pomeau-Pazzis) and hexagonal grid model FHP (Frisch-Hasslacher-Pomeau) (Rivet & Boon 2001). To bring the usually complex physical domain of interest under control, the LBM had to resolve two challenging obstacles. The first concerns the calculation grid, which needs to fit any given physical domain. The second problem is related to the definition of boundary conditions along the solid boundary. Employing experience gained by traditional computational fluid dynamics (finite difference, finite element method) seemed to offer the most obvious solution: transformation of partial differential equations of flow in a curvilinear coordinate system and solving them by adequate numerical methods. For example, Mei & Shyy (1998), Guo & Zhao (2003) and Li *et al.* (2008) have used the finite difference method for modeling the

doi: 10.2166/hydro.2012.097

lattice Boltzmann partial differential equations transformed in curvilinear coordinates. Peng *et al.* (1998), Ubertini *et al.* (2003), Joshi *et al.* (2009) and Stiebler *et al.* (2006) made use of the finite volume method in cases of physical domains having complex geometry. However, combined with classical computation techniques, the resulting method also suffered from the problems of classical numerical procedures, related to the choice of the most suitable finite difference approximation of equations and their solutions. At the same time, the most significant advantages of the Boltzmann method, simplicity and efficiency, were lost. In order to maintain these advantages when modeling complex physical domains, He *et al.* (1996) and He & Doolen (1997) have proposed, and Lu *et al.* (2002) and Cheng & Hung (2004) applied successfully, the interpolation supplemented method. In the case of a non-uniform grid this procedure utilizes the basic Lagrangian nature of the LBM combined with the interpolation of unknown dependent variables in the calculation nodes. However, the drawbacks of this approach include significantly increased demand for computational resources and the introduction of numerical distortion into the solution via the interpolation procedure itself. For that, Shu *et al.* (2002) and Shu *et al.* (2001) recommended an application of Taylor-series expansion and the least-squares approach, subsequently modified by Han *et al.* (2007). Not even this could completely eliminate the need for additional calculation steps thereby adversely influencing the basic LBM. Inspired by the paper of Koelman (1991), Bouzidi *et al.* (2001) presented the multiple relaxation time (MRT) LBM for a 2D rectangular mesh. Subsequently Zhou (2010) adapted this type of mesh to the standard Lattice Bhatnagar-Gross-Krook (LBGK) method by correcting the equilibrium function. Besides the mentioned procedures, models based on local mesh refinement are often used. Procedures for determining the unknown distribution functions along the boundaries between the finer and coarser grid have been proposed first by Filippova & Hänel (1998), modified and improved later by Lin & Lai (2002), and Dupuis & Chopard (2003). Application of these procedures can be found in Yu *et al.* (2002) and Liu *et al.* (2009).

As mentioned earlier, modeling flow with LBM in cases of physical domains having arbitrary geometry, where the boundaries of the domain hardly ever fit the principle directions of calculation, a proper definition of conditions along the solid boundaries emerges. A significant advantage of the LBM in flow modeling is that in cases of flow domains having regular shape, setting the boundary conditions is very straightforward. So for no-slip boundary conditions, the bounce-back method is applied, while for slip boundary conditions the elastic-collision scheme is utilized (Rothman & Zaleski 1997; Rivet & Boon 2001; Zhou 2004). However, if the boundary intersects with the calculation mesh at an arbitrary angle, the definition of unknown particle distribution functions requires further considerations. Filippova & Hänel (1998) introduced a procedure for generating a particle distribution function 'coming' from a 'solid' node to the corresponding 'wet' node. Mei *et al.* (1999) succeeded in improving its stability to some extent. Using linear interpolation to define the unknown distribution functions in the vicinity of the boundary, Yu *et al.* (2003) have eliminated the need for using different interpolation functions depending on node position. The limitation and drawback of the proposed procedures lie first of all in assuming low flow velocities, making them applicable in steady state cases only. Inspired by Chen *et al.* (1996), Guo *et al.* (2002) suggested splitting the unknown particle distribution function to its equilibrium and non-equilibrium parts and extrapolating the unknown fictive velocity to the wall node. In order to improve accuracy in the calculation of velocities near to the solid boundary (consequently over the whole calculation domain as well), Kang *et al.* (2008) applied a suitable dynamic equation to the wall nodes in order to determine the fictive velocities in them. Based on the work of Lätt *et al.* (2008), Verschaeve & Müller (2010) came up with an approach of reconstructing the unknown particle distribution function using density, velocity and rate of strain. To avoid needing to know the parameters in the nodes neighboring the boundary nodes, Lee & Lee (2010) suggested using a non-uniform calculation grid along the boundary region. A better fitting of calculation mesh to the boundary of the physical domain is achievable via shifting the position of 'wet' nodes by changing the dimensions of the calculation cells. It can be concluded that modeling arbitrarily shaped physical domains with the

corresponding boundary conditions by means of the LBM is still in an experimental phase dealing with complicated and impractical procedures of unsatisfactory accuracy. Domains of complex geometry are covered with classical rectangular meshes which require producing additional, complicated and demanding expressions to enable the arrangement of boundary conditions along the solid boundary. Consequently this noticeably influences the accuracy of the solution, as well the efficiency and simplicity of the LBM. For this the LBM still is not suitable for practical application in the field of river hydraulics or in modeling lake processes, i.e. modeling in domains of natural geometry.

In order to overcome problems linked to modeling flow in environments of complex shape, furthermore to extend practical applicability of the LBM, this paper is aimed at presenting LBM for modeling equations of 2D flow completely transformed in curvilinear coordinates. The physical domain of interest is covered by a curvilinear mesh which fits to the contours of the domain easily. Following the metrics of transformation between the physical and calculation, domain was established. As in a 2D case where the calculation domain is rectangular, the basic mesh of the LBM was utilized for this purpose. Following the establishment of metrics, transformation of equations of 2D flow in curvilinear coordinates was accomplished. Finally, definition of equilibrium functions was undertaken. Since the complete calculation is performed in the basic LBM environment, the resulting method preserves the simplicity and efficiency of the basic LBM. This applies to the calculation mesh as well as to the boundary conditions along the solid boundary, for which the original form of bounce-back and elastic-collision schemes are relevant, not requiring additional terms. This approach completely eliminates the likelihood of introducing errors into the formulation of the unknown particle distribution functions close to the solid boundary. As a result, the accuracy of the calculation is further improved near to the boundary, as well as over the whole calculation domain. The potential of the proposed procedure is demonstrated through three examples, all having a complex geometry of the physical domain. The results are presented in combination with the verification of the model.

THE MATHEMATICAL MODEL

Complete transformation of shallow water equations in a curvilinear coordinate system

Shallow water equations in Cartesian coordinates (x, y) are:

$$\frac{\partial h}{\partial t}+\frac{\partial (hu)}{\partial x}+\frac{\partial (hv)}{\partial y}=0, \tag{1}$$

$$\frac{\partial (hu)}{\partial t}+\frac{\partial (hu^2)}{\partial x}+\frac{\partial (huv)}{\partial y}=-gh\frac{\partial Z_b}{\partial x}-\frac{g}{2}\frac{\partial h^2}{\partial x}-\frac{\tau_{bx}}{\rho}+\frac{\tau_{wx}}{\rho}+\frac{\tau_{fx}}{\rho}+\nu\frac{\partial^2 (hu)}{\partial x^2}+\nu\frac{\partial^2 (hu)}{\partial y^2}+fhv, \tag{2}$$

$$\frac{\partial (hv)}{\partial t}+\frac{\partial (huv)}{\partial x}+\frac{\partial (hv^2)}{\partial y}=-gh\frac{\partial Z_b}{\partial y}-\frac{g}{2}\frac{\partial h^2}{\partial y}-\frac{\tau_{by}}{\rho}+\frac{\tau_{wy}}{\rho}+\frac{\tau_{fy}}{\rho}+\nu\frac{\partial^2 (hv)}{\partial x^2}+\nu\frac{\partial^2 (hv)}{\partial y^2}-fhu, \tag{3}$$

where x, y are the Cartesian coordinates, u, v are the Cartesian components of the flow velocity, h is the water depth, z_b is the bed level, τ_{bx}, τ_{by} are the bottom shear stresses, τ_{wx}, τ_{wy} are the shear stresses due to wind forcing, τ_{fx}, τ_{fy} are the shear stresses along the solid boundary (Zhou 2004), ρ is the water density, f is the Coriolis parameter and ν is the coefficient of kinematic viscosity. By establishing the transfer function between the physical and calculation domain, $x=f(\xi, \eta)$, $y=f(\xi, \eta)$, (Figure 1), and applying the rules of complete transformation (Simmonds 1994) to Equations (1), (2) and (3), in a curvilinear coordinate system (ξ, η) they become:

$$\frac{\partial (J^2 h)}{\partial t}+\frac{\partial (J^2 hU)}{\partial \xi}+\frac{\partial (J^2 hV)}{\partial \eta}=JhU\frac{\partial J}{\partial \xi}+JhV\frac{\partial J}{\partial \eta}, \tag{4}$$

$$\frac{\partial (J^2 hU)}{\partial t}+\frac{\partial (J^2 hU^2)}{\partial \xi}+\frac{\partial (J^2 hUV)}{\partial \eta}=-\frac{g}{2}\frac{\partial}{\partial \xi}(G_{22}h^2)+\nu\frac{G_{22}}{J^2}\frac{\partial^2 (J^2 hU)}{\partial \xi^2}+\nu\frac{G_{11}}{J^2}\frac{\partial^2 (J^2 hU)}{\partial \eta^2}+E_\xi+D_\xi, \tag{5}$$

$$\frac{\partial (J^2 hV)}{\partial t}+\frac{\partial (J^2 hUV)}{\partial \xi}+\frac{\partial (J^2 hV^2)}{\partial \eta}=-\frac{g}{2}\frac{\partial}{\partial \eta}(G_{11}h^2)+\nu\frac{G_{22}}{J^2}\frac{\partial^2 (J^2 hV)}{\partial \xi^2}+\nu\frac{G_{11}}{J^2}\frac{\partial^2 (J^2 hV)}{\partial \eta^2}+E_\eta+D_\eta. \tag{6}$$

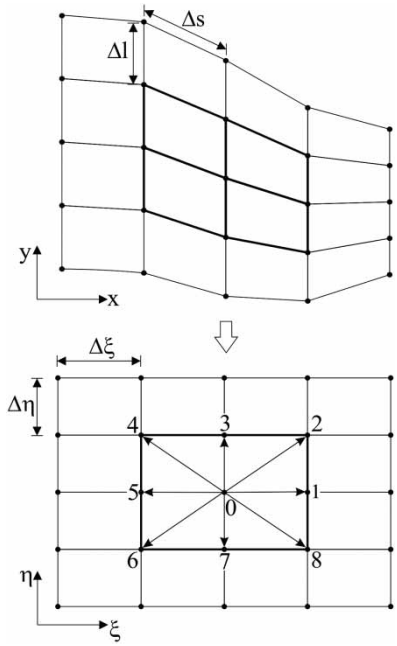

Figure 1 | The physical domain and the corresponding rectangular lattice (D2Q9).

In the transformed expressions, Equations (4), (5) and (6), ξ, η are the curvilinear coordinates, U, V are the contravariants of the velocity, $J = x_\xi y_\eta - x_\eta y_\xi$ is the determinant of the Jacobian matrix, x_ξ, y_ξ, x_η, y_η are the geometric derivatives (basis vectors), $G_{11} = (x_\xi)^2 + (y_\xi)^2$, $G_{22} = (x_\eta)^2 + (y_\eta)^2$ and $G_{12} = x_\xi x_\eta + y_\xi y_\eta$ are the metric coefficients of transformation. Terms E and D include the remainder of transformed equations concerning advection, pressure, surface and bottom shear stresses, shear stress along the solid boundary, Coriolis forces and the remaining terms of the transformed part of diffusion, respectively:

$$E_\xi = Jhu^2\frac{\partial}{\partial\eta}\left(\frac{v}{u}\right) + J^2hV^2\frac{\partial}{\partial\eta}\left(\frac{U}{V}\right) + \frac{g}{2}h^2\frac{\partial G_{22}}{\partial\xi} + gh\left[-G_{22}\frac{\partial Z_b}{\partial\xi} + G_{12}\left(\frac{\partial Z_b}{\partial\eta} + \frac{\partial h}{\partial\eta}\right)\right] + Jy_\eta\left(\frac{\tau_{wx}}{\rho} - \frac{\tau_{bx}}{\rho} + \frac{\tau_{fx}}{\rho}\right) - Jx_\eta\left(\frac{\tau_{wy}}{\rho} - \frac{\tau_{by}}{\rho} + \frac{\tau_{fy}}{\rho}\right) + Jfh(UG_{12} + VG_{22}), \quad (7)$$

$$D_\xi = \frac{\partial}{\partial\xi}\left(\frac{\nu G_{22}}{J^2}\right)\frac{\partial}{\partial\xi}(J^2hU) + \frac{\partial}{\partial\eta}\left(\frac{\nu G_{11}}{J^2}\right)\frac{\partial}{\partial\eta}(J^2hU) - \frac{\partial}{\partial\xi} \times \left(\frac{\nu G_{22}hU}{J}\frac{\partial J}{\partial\xi}\right) - \frac{\partial}{\partial\eta}\left(\frac{\nu G_{11}hU}{J}\frac{\partial J}{\partial\eta}\right) - \frac{\partial}{\partial\xi}\left(\frac{\nu G_{12}}{J}\frac{\partial}{\partial\eta}(JhU)\right) - \frac{\partial}{\partial\eta}\left(\frac{\nu G_{12}}{J}\frac{\partial}{\partial\xi}(JhU)\right) + \frac{\partial(hu)}{\partial\xi}\frac{\nu}{J}\left(G_{12}\frac{\partial y_\eta}{\partial\eta} - G_{22}\frac{\partial y_\eta}{\partial\xi}\right) + \frac{\partial(hu)}{\partial\eta}\frac{\nu}{J}\left(G_{12}\frac{\partial y_\eta}{\partial\xi} - G_{11}\frac{\partial y_\eta}{\partial\eta}\right) + \frac{\partial(hv)}{\partial\xi}\frac{\nu}{J} \times \left(G_{22}\frac{\partial x_\eta}{\partial\xi} - G_{12}\frac{\partial x_\eta}{\partial\eta}\right) + \frac{\partial(hv)}{\partial\eta}\frac{\nu}{J}\left(G_{11}\frac{\partial x_\eta}{\partial\eta} - G_{12}\frac{\partial x_\eta}{\partial\xi}\right). \quad (8)$$

Corresponding expressions for E_η and D_η are given in Appendix A (available online at http://www.iwaponline.com/jh/014/097.pdf).

The lattice Boltzmann method

For modeling the equations of 2D flow transformed in a curvilinear coordinate system (4–8 and A1–A2), the 2D LBM for rectangular lattice (D2Q9) proposed by Zhou (2010) is adopted in this work. Since square or rectangular lattices are considered, the evolution of distribution function of particles is given by the lattice Boltzmann equation as:

$$f_\alpha(\varsigma + e_\alpha\Delta t, t + \Delta t) = f_\alpha(\varsigma, t) + \frac{1}{\tau}(f_\alpha - f_\alpha^{eq}) + F_\alpha\Delta t. \quad (9)$$

To be applicable on a rectangular lattice, where dimensions $\Delta\xi$ and $\Delta\eta$ of the lattice are unequal (Figure 1), the discretized velocity of particles, e_α in case of rectangular lattice type D2Q9 is defined as:

$$e_\alpha = \begin{bmatrix} (0, 0), & \alpha = 0 \\ (\pm e_\xi, 0), & \alpha = 1, 5 \\ (0, \pm e_\eta), & \alpha = 3, 7 \\ (\pm e_\xi, \pm e_\eta), & \alpha = 2, 4, 6, 8, \end{bmatrix} \quad (10)$$

where $e_\xi = \Delta\xi/\Delta t$ and $e_\eta = \Delta\eta/\Delta t$ are the components of velocity e_α in directions ξ and η, $\Delta\xi$ and $\Delta\eta$ are the lattice sizes in ξ and η directions, f_α is the distribution function of particles in the α link, f_α^{eq} is the local equilibrium distribution function, ζ is the position vector in the 2D curvilinear domain given as $\zeta = (\xi, \eta)$, t is time and Δt is the time step. As can be seen from Equation (10), the difference in adopting a lattice having a length/width ratio different from one, compared to the case of a classical square lattice, is in different particle velocity components depending on the direction of the α link. Examples concerning application of the LBM on rectangular lattices, both for physical domains of regular and complex shape, can be found in Zhou (2010).

The next step in the creation of a lattice Boltzmann model with Equation (9) is to define appropriate local

equilibrium distribution functions. Detailed theory supporting LGA and LBM is outlined in Zhou (2004), Rivet & Boon (2001) and Rothman & Zaleski (1997). Differing from the classical approach of modeling domains of complex geometry utilizing classical equations of flow in Cartesian coordinates, equations transformed in a curvilinear coordinate system are used here, Equations (4)–(8) and Equations (A1)–(A2). According to this and regarding the local equilibrium distribution function as given in (Zhou 2010), the following form of f_α^{eq} is suggested here:

$$f_\alpha^{eq}=\begin{cases} J^2\,h-\sum\limits_{i=1}^{8} f_\alpha^{eq}, & \alpha=0 \\ \left(G_{22}\dfrac{gh}{4e_\xi^2}+\dfrac{J^2U}{3e_{a\xi}}+\dfrac{J^2U^2}{2e_\xi^2}\right)h, & \alpha=1,5 \\ \left(G_{11}\dfrac{gh}{4e_\eta^2}+\dfrac{J^2V}{3e_{a\eta}}+\dfrac{J^2V^2}{2e_\eta^2}\right)h, & \alpha=3,7 \\ \left(\dfrac{J^2U}{12e_{a\xi}}+\dfrac{J^2V}{12e_{a\eta}}+\dfrac{J^2UV}{4e_{a\xi}e_{a\eta}}\right)h, & \alpha=2,4,6,8, \end{cases} \tag{11}$$

while the force term is given as:

$$F_\alpha=\begin{cases} JhU\dfrac{\partial J}{\partial\xi}+JhV\dfrac{\partial J}{\partial\eta}, & \alpha=0 \\ \dfrac{(E_\xi+D_\xi)}{6e_{a\xi}}, & \alpha=1,5 \\ \dfrac{(E_\eta+D_\eta)}{6e_{a\eta}}, & \alpha=3,7 \\ \dfrac{(E_\xi+D_\xi)}{6e_{a\xi}}+\dfrac{(E_\eta+D_\eta)}{6e_{a\eta}}, & \alpha=2,4,6,8. \end{cases} \tag{12}$$

It can be shown that an application of the Chapman-Enskog procedure (Rothman & Zaleski 1997; Rivet & Boon 2001; Zhou 2004, 2010) on Equation (9), where physical variables are given as:

$$h=\frac{1}{J^2}\sum_{\alpha=0}^{8} f_\alpha,\ U=\frac{1}{J^2\,h}\sum_{\alpha=0}^{8} e_{a\xi}f_\alpha,\ V=\frac{1}{J^2\,h}\sum_{\alpha=0}^{8} e_{a\eta}f_\alpha, \tag{13}$$

and the force term is:

$$\begin{aligned} &\sum_{\alpha=0}^{8} F_\alpha=JhU\frac{\partial J}{\partial\xi}+JhV\frac{\partial J}{\partial\eta}, \\ &\sum_{\alpha=0}^{8} e_{a\xi}F_\alpha=E_\xi+D_\xi,\ \sum_{\alpha=0}^{8} e_{a\eta}F_\alpha=E_\eta+D_\eta, \end{aligned} \tag{14}$$

results in transformed shallow water Equations (4)–(8) and (A1)–(A2) as presented earlier. Regarding the character of the diffusive terms, the following approximation of the kinematic viscosity is adopted:

$$\nu=\frac{1}{2}\left(\frac{J^2}{G_{22}}+\frac{J^2}{G_{11}}\right)\frac{e_\xi e_\eta\Delta t}{6}(2\tau-1.0). \tag{15}$$

Equation (15) suggests that a single value for the kinematic viscosity is achievable only if J^2/G_{22} equals J^2/G_{11}. This criterion is fulfilled if the dimension ratio of the curvilinear mesh, $\Delta s/\Delta l$ is equal to the dimension ratio of the lattice, $\Delta\xi/\Delta\eta$. By this, an equivalence of terms J^2/G_{22} and J^2/G_{11} is theoretically achieved; however they are seldom equivalent in practice. Averaging the two close values overrides the problem, giving a single nominal value.

According to Equations (5) and (6), geometrical coefficients G_{11}, G_{22}, G_{12} and J depend on independent parameters ξ and η only. Their values need to be calculated once only, prior to proceeding along to the main calculation course. Consequently, for a constant value of kinematic viscosity the resulting relaxation time is also a function of independent parameters ξ and η only:

$$\tau(\xi,\eta)=\nu\frac{1}{J(\xi,\eta)^2}(G_{22}(\xi,\eta)+G_{11}(\xi,\eta))\frac{1.5}{e_\xi e_\eta\Delta t}+\frac{1}{2}, \tag{16}$$

An analogous procedure to that used for transforming shallow water equations in a curvilinear coordinate system and modeling by LBM is applicable to the 2D (in the horizontal plane) Navier-Stokes equations as well. Accordingly, the equilibrium function f_α^{eq} and the force term F_α of the transformed 2D Navier-Stokes equations in a curvilinear coordinate system take the form:

$$f_\alpha^{eq}=\begin{cases} J^2\rho-\sum\limits_{i=1}^{8} f_\alpha^{eq}, & \alpha=0 \\ \left(G_{22}\omega\dfrac{e_\eta}{e_\xi}+\dfrac{J^2U}{3e_{a\xi}}+\dfrac{J^2U^2}{2e_\xi^2}\right)\rho, & \alpha=1,5 \\ \left(G_{11}\omega\dfrac{e_\xi}{e_\eta}+\dfrac{J^2V}{3e_{a\eta}}+\dfrac{J^2V^2}{2e_\eta^2}\right)\rho, & \alpha=3,7 \\ \left(\dfrac{J^2U}{12e_{a\xi}}+\dfrac{J^2V}{12e_{a\eta}}+\dfrac{J^2UV}{4e_{a\xi}e_{a\eta}}\right)\rho, & \alpha=2,4,6,8, \end{cases} \tag{17}$$

and:

$$F_\alpha = \begin{cases} J\rho U\dfrac{\partial J}{\partial \xi} + J\rho V\dfrac{\partial J}{\partial \eta}, & \alpha = 0 \\ \dfrac{(E_\xi + D_\xi)}{6e_{\alpha\xi}}, & \alpha = 1, 5 \\ \dfrac{(E_\eta + D_\eta)}{6e_{\alpha\eta}}, & \alpha = 3, 7 \\ \dfrac{(E_\xi + D_\xi)}{6e_{\alpha\xi}} + \dfrac{(E_\eta + D_\eta)}{6e_{\alpha\eta}}, & \alpha = 2, 4, 6, 8. \end{cases} \quad (18)$$

The corresponding transformed Navier-Stokes equations of flow are given in Appendix B (available online http://www.iwaponline.com/jh/014/097.pdf). In the suggested Equation (18) parameter ω, defined by Zhou (2010) as:

$$\omega < \min\left\{\frac{\Delta\xi}{\Delta\eta}, \frac{\Delta\eta}{\Delta\xi}\right\} \leq 1.0, \quad (19)$$

controls stability. Applying the Chapman-Enskog analysis on Equation (9), using local equilibrium distribution function (17) and force term F_α given by (18) modeled with a centered scheme (Zhou 2004), it can be demonstrated that pressure p depends on density as $p = 2\rho\omega e_\xi e_\eta$.

In order to verify the proposed form of LBM for modeling flow equations transformed in curvilinear coordinates, the transformed shallow water equations were tested on three examples having different geometries. The first example is a straight prismatic channel angled 45° to the main axes. The second is a pool of circular shape in the base plot. The third example is a prismatic flume with a 180° bend. In the case of the first two test examples, the results obtained by the described numerical approach were compared with the corresponding analytical solutions, while appropriate measurements represented reference in the third case.

MODEL TESTING AND VERIFICATION

Mathematical modeling of flows in domains having natural geometry, often associated with very complex boundary conditions, is a remarkable challenge in current hydraulic practice. Classical rectangular meshes are hardly ever suitable for describing domains of complex geometry and modeling the corresponding flow patterns. Partly due to the problems associated with describing complex physical domains with orthogonal rectangular meshes, and partly because of impracticality of applying boundary conditions in such environments, orthogonal meshes are replaced by equivalent curvilinear ones, while the calculations are still performed in a rectangular grid. The lattice Boltzmann model with the transformed shallow water equations outlined earlier has been tested on three particular test examples.

Straight prismatic channel angled 45° to the main axes

As pertaining to the order of checking the results of the proposed procedure against a simple analytical solution, while all elements of the equations transformed in the curvilinear coordinate system become activated, the case of a straight prismatic channel of rectangular cross section positioned diagonally has been considered as the first. A channel of width $B = 0.8$ m and length $L = 4.0$ m was covered by mesh having elements $\Delta s = 0.04$ m and $\Delta l = 0.02$ m (Figure 2).

Establishing the metrics linking the physical and calculation domain, which means determining the values of coefficients G_{11}, G_{22}, G_{12} and J, where the geometric derivatives x_ξ, y_ξ, x_η and y_η are approximated with finite differences of second order (central dif.), is a precondition for the next step, setting the boundary conditions. In this example the adopted lattice sizes are $\Delta\xi = 0.04$ and $\Delta\eta = 0.02$. In the most upstream cross section, a discharge of $Q = 0.0123$ m^3

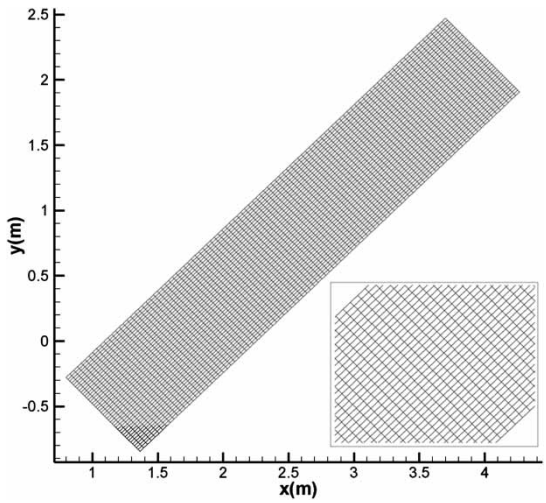

Figure 2 | The mesh adopted for the diagonally placed straight channel of rectangular cross section.

s^{-1} has been set associated with a constant depth of $h = 0.1$ m at the most downstream end of the channel. In accordance with parameters $\Delta\xi$ and $\Delta\eta$, a rectangular lattice 101×41 has been implemented. The value of $\nu = 0.03\ m^3\ s^{-1}$ for the kinematic viscosity and the chosen time step of $\Delta t = 0.014$ s according to Equation (16) resulted in a relaxation time $\tau = 2.07$ for the whole domain. Written in the form of the lattice Boltzmann model, the upstream boundary condition becomes:

$$f_\alpha(\xi, \eta) = f_\alpha(\xi + \Delta\xi, \eta), \quad \alpha = 1, 2, 8, \tag{20}$$

while the velocity gradient equal to zero at the downstream end is written as:

$$f_\alpha(\xi, \eta) = f_\alpha(\xi - \Delta\xi, \eta), \quad \alpha = 5, 4, 6. \tag{21}$$

Since the calculation is carried out in classical rectangular lattices, a no-slip condition realized through the bounce-back procedure has been set as the boundary condition along the solid boundary.

In Figures 3 and 4 the numerical solution in the form of velocity distribution across the channel is compared to the analytical solution given by:

$$u(s) = u_0\left(1.0 - \left(\frac{s - s_0}{s_0}\right)^2\right), \tag{22}$$

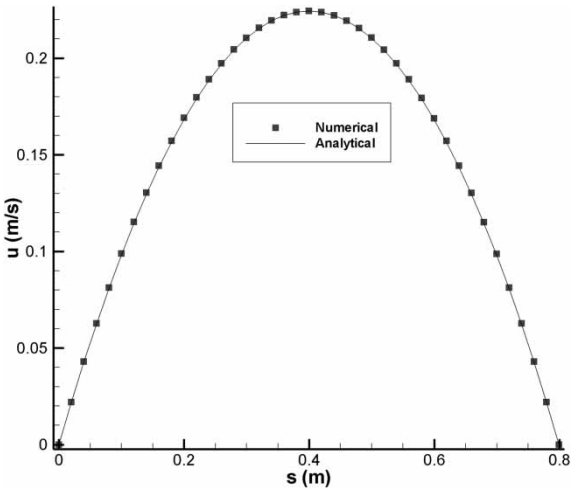

Figure 3 | Numerical solution of the LBM compared to the analytical.

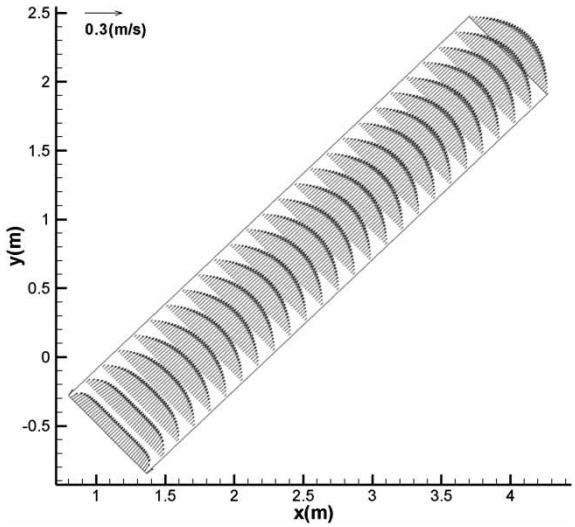

Figure 4 | Flow pattern in a diagonally placed prismatic channel calculated by the LBM.

where s is distance measured from the left bank of the channel in the Cartesian domain.

As seen in Figure 3 the numerical solution obtained by the proposed LBM fully coincides with the analytical.

Pool of circular shape in base plot

The second example for testing the suitability of the suggested LBM for modeling shallow water equations transformed in curvilinear coordinates is a more demanding circular shape pool. This pool represents a simplified pond having bottom levels relative to the water level given by Kranenburg (1992) as:

$$Z_b = 1 - \frac{1}{1.3}\left(\frac{1}{2} + \sqrt{\frac{1}{2} - \frac{1}{2}\frac{r}{R_0}}\right), \tag{23}$$

where r is the distance from the center of the pond and $R_0 = 194.0$ m is the radius of the pond edge.

As can be seen in Figure 5 showing the applied curvilinear mesh having a central cell of dimensions $\Delta s = 6.5$ m and $\Delta l = 6.5$ m, the deformation of the mesh is significant, increasing from the center towards the edge of the domain. Critical degrees of deformation are reached in just four points located along the edge of the pool, characterized by extremely high values of parameters J^2/G_{22} and J^2/G_{11}. This deteriorates the stability of the LBM. In order to get

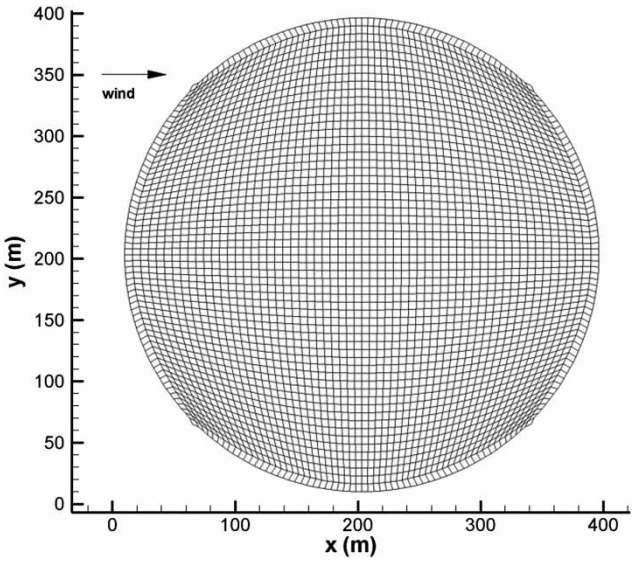

Figure 5 | The curvilinear mesh adopted for the circular pool.

rid of the potential causes of instability, only at these locations has the mesh been slightly modified. In the mentioned four points, the outer sides of the calculation cell cross each other at an angle of about 180°, consequently some of the geometric derivatives x_ξ, y_ξ, x_η, y_η tend towards zero. Inserted into the metric coefficients and the Jacobian, instability is provoked. This is not special to the LBM only, but characteristic of FDM methods as well. Instability can be avoided by dislocating slightly the problematic corner of the calculation mesh ensuring the angle between the sides of the problematic is not 180°. This will not affect the results significantly. The appropriate measure of dislocation (the slightest dislocation giving a stable calculation scheme) should be determined by trial and error approach.

Subsequently a west wind producing shear stresses of $\tau_{wx} = 4.0\ \mathrm{Nm}^{-2}$ and $\tau_{wy} = 0.0\ \mathrm{Nm}^{-2}$ has been applied to the surface of the pond. In order to produce a numerical solution comparable to the analytical solution given by Kranenburg (1992) as:

$$u = u_* \left(\frac{h}{H} - 1 \right) \cdot \frac{\ln(Z)}{\kappa}, \tag{24}$$

where h is the water depth, $H = 1/1.3$ is the weighted averaged water depth, $u_* = \sqrt{\tau_w/\rho}$ is the friction velocity at the free surface, $Z = H/z_0$ and $z_0 = 2.8$ mm are the roughness heights and $\kappa = 0.4$ is the von Kármán constant, the bottom shear stress, τ_{bx}, τ_{by} and the shear stress along the solid boundary, τ_{fx}, τ_{fy}, have been set to zero. Furthermore, since the complete calculation is carried out in the basic form of rectangular lattices, lattice sizes $\Delta\xi = 2.0$ and $\Delta\eta = 2.0$ have been chosen, resulting in 61×61 rectangular lattices. In accordance with the analytical solution (24), the slip condition in its basic simple form has been applied to the solid boundary. The time step was $\Delta t = 0.2$ s. The numerical solution in the form of streamlines is given in Figure 6. Comparison of the numerical solution to the analytical in the form of normalized depth-averaged velocity profiles, $\kappa u_k/(u_* \ln Z)$ across the pool along the axis normal to the wind direction s_r is given in Figure 7. In the case of the analytical solution, velocity u_k is given by Equation (24) while in the numerical solution u_k is defined as $u_k = ((u+v)/|u+v|)\sqrt{u^2+v^2}$.

The calculated flow pattern given in Figure 6 is in full agreement with the expected wind-generated patterns occurring in ponds; the flow pattern is symmetrical, the flow direction near to the pond's edge coincides with the wind direction, while it is opposite along the axis of symmetry. Incidence of such flow patterns by wind force is a basic feature of lakes and ponds. Moreover, the solution of shallow water equations in curvilinear coordinates by LBM is in significant agreement with the analytical solution, Figure 7. A similar comparison is outlined in Zhou

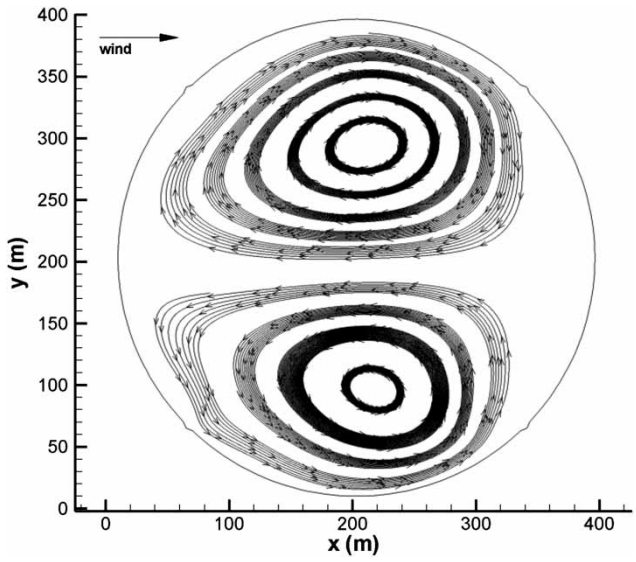

Figure 6 | The calculated flow pattern generated by the west wind.

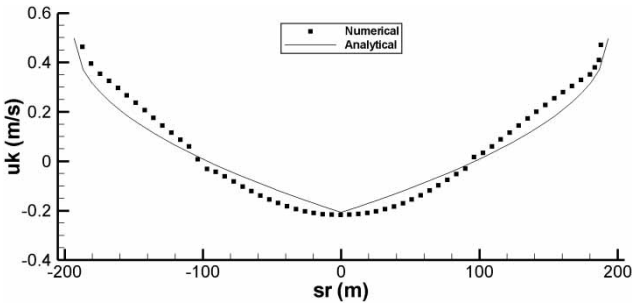

Figure 7 | Comparison of the numerical LBM solution to the analytical.

(2004), where the numerical LBM close to the boundary produced a certain disagreement with the analytical solution. In this particular critical region, significant improvement has been achieved with the LBM procedure proposed here. This improvement is mainly the consequence of modeling the transformed equations of flow, which ensure formulation of the problem in an environment more fitting to the investigated physical domain. By this the basic parameters of flow (velocity components) and the processes involved acquire a more natural form. Application of the proposed LBM procedure completely eliminates the need for additional expressions or procedures in the near-boundary region in cases of complex-shape domains. The basic form of boundary condition modeling is applied, resulting in an increase of accuracy even in the critical regions.

Prismatic flume in a 180° bend

As mentioned previously, the aim of mathematical modeling is in defining, studying and calculating processes in domains 'as given'. Consequently, the mathematical model needs to be checked not just for relatively simple cases for which an analytical solution is available, but also for more complex and relevant examples obtained by laboratory or field measurements. For this, the third test example is a prismatic laboratory flume in a 180° bend, namely it is test No. 8 of Rozovskii (1963) which has already become a standard in testing numerical models.

It is a $B = 0.8$ m wide prismatic laboratory flume of rectangular cross section, consisting of three segments. The most upstream segment is a 6.0 m long straight part, followed by the second segment with a circular bend of 180° having a centerline radius of 0.8 m. The third, most downstream segment is also straight but only 3 m long (Figure 8). With respect to the requirement of equal values for coefficients J^2/G_{22} and $J^2/G1$ declared earlier, the straight portions of the above described flume were covered by a mesh of dimensions $\Delta s = 0.04$ m and $\Delta l = 0.02$ m. Mesh dimensions are $\Delta s = 0.0605$ m and $\Delta l = 0.03025$ m along the concave side of the bend, while $\Delta s = 0.0203$ m and $\Delta l = 0.0102$ m on the convex side. The resulting curvilinear mesh made up of 288×41 calculation cells is shown in Figure 8.

Next, the appropriate boundary conditions have been set to the numerical model, complying with the physical model. At the upstream end, a constant discharge of $Q = 0.0123\ \mathrm{m^3\ s^{-1}}$ and depth gradient equal to zero have been set, $\partial h/\partial \xi = 0.0$. On the downstream end, a constant depth $h = 0.05$ m and a velocity gradient perpendicular to the cross section equal to zero has been applied, $\partial U/\partial \xi = 0.0$. Since the bottom shear stresses, τ_{bx}, τ_{by} were modeled by Manning's equation,

$$\tau_{bx} = \frac{gn^2}{(h^{1/3})}\rho U\sqrt{U^2G_{11} + 2UVG_{12} + V^2G_{22}},$$
$$\tau_{by} = \frac{gn^2}{(h^{1/3})}\rho V\sqrt{U^2G_{11} + 2UVG_{12} + V^2G_{22}}. \quad (25)$$

Chezy's coefficient of friction resistance has been set to $C = 32$. This resulted in Manning's coefficient of $n = 0.023\ \mathrm{m^{-1/3}\ s^{-1}}$. A similar expression was assumed for the

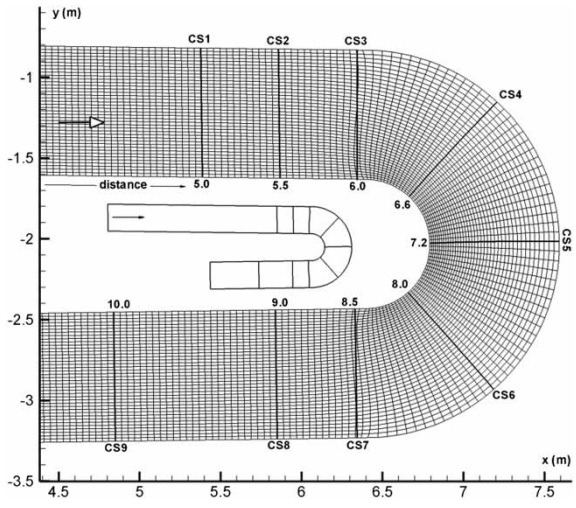

Figure 8 | The curvilinear mesh adopted for modeling the flume in a 180° bend.

friction stresses, τ_{fx}, τ_{fy} along the solid boundary:

$$\tau_{fx} = -C_f \rho U \sqrt{U^2 G_{11} + 2UVG_{12} + V^2 G_{22}},$$
$$\tau_{fy} = -C_f \rho V \sqrt{U^2 G_{11} + 2UVG_{12} + V^2 G_{22}}, \quad (26)$$

where $C_f = 3.75$ has been agreed upon. In accordance with the friction stresses τ_{fx}, τ_{fy} modeled along the solid boundary, the slip condition has been applied by the original elastic-collision scheme. Accordingly, the unknown particle distribution function was determined in its familiar form:

$$f_2 = f_8,\ f_3 = f_7,\ f_4 = f_6. \quad (27)$$

In addition to the flow parameters, setting up LBM for the shallow water equations in curvilinear coordinates requires establishing the metrics between the physical and calculation domains. Lattice sizes $\Delta\xi = 0.02$ and $\Delta\eta = 0.01$ adopted for this purpose resulted in 288×41 rectangular lattices in the entire calculation domain. For the chosen value of kinematic viscosity $\nu = 0.0165\ \mathrm{m^2\ s^{-1}}$ and time step $\Delta t = 0.014$ s, the relaxation time $\tau(\xi, \eta)$ is determined by Equation (16) in the domain of interest. This parameter is constant along the straight segments having values of $\tau = 1.367$. The relaxation time changes from its minimum value of $\tau = 0.858$ on the concave side to its maximum $\tau = 3.535$ on the inner, convex side of the bend.

Since the calculation started with a state of no flow along the flume (all velocities set to zero), steady state flow conditions have been established after about 6,000 calculation steps. The resulting flow pattern is shown in Figure 9. Furthermore, in order to verify the water levels calculated by the curvilinear LBM, a comparison of the calculated water level distribution with the experimental results is presented in Figure 10. It is to be mentioned that the levels in Figure 10 are reduced by the minimum depth (observed in the most downstream cross section) to comply with the presentation of experimental results as given in Rozovskii (1963). Figure 11 shows the comparison of calculated and measured (averaged along the vertical axis) tangential velocities, in cross sections *CS1–CS9* positioned as shown in Figure 8. In Figure 11, s is the distance from the inner, convex bank of the flume measured in radial direction.

As demonstrated by Figures 10 and 11, the proposed form of the LBM for the shallow water equations

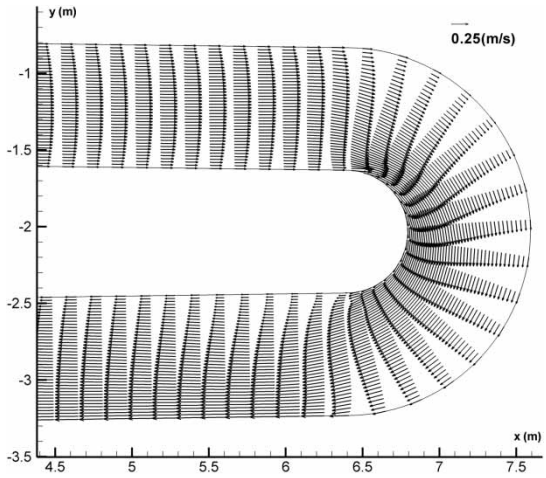

Figure 9 | Flow pattern in a prismatic flume bent 180°, calculated with LBM.

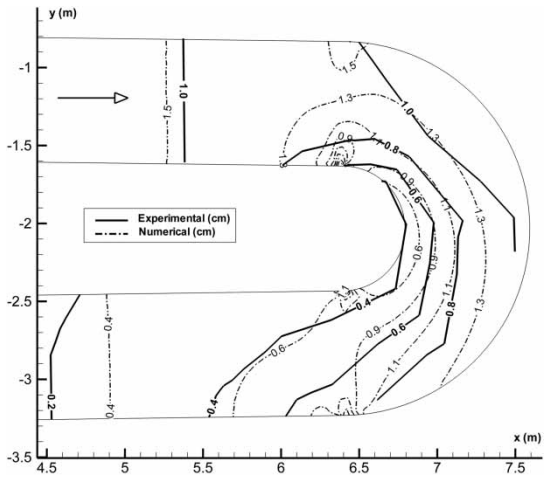

Figure 10 | Water levels measured in a laboratory flume and calculated by the LBM.

transformed in curvilinear coordinates shows a very high level of accuracy, even with flows having 3D characteristics like that in the flume with a 180° bend. The curvilinear LBM has been compared with the Cartesian LBM, applied to the same example, published in Zhou (2004, 2010). He has covered the calculation domain by 400×125 square lattices with $\Delta x = \Delta y = 0.0200$ m, and reached steady state solution after 5,000 iterations. The curvilinear LBM has produced better results in all cross sections (Figure 11). Very good agreement is evident not only over the central region of the flow but even in the most critical regions near to the solid boundaries. Major differences between the measured and calculated tangentional velocities appear along the

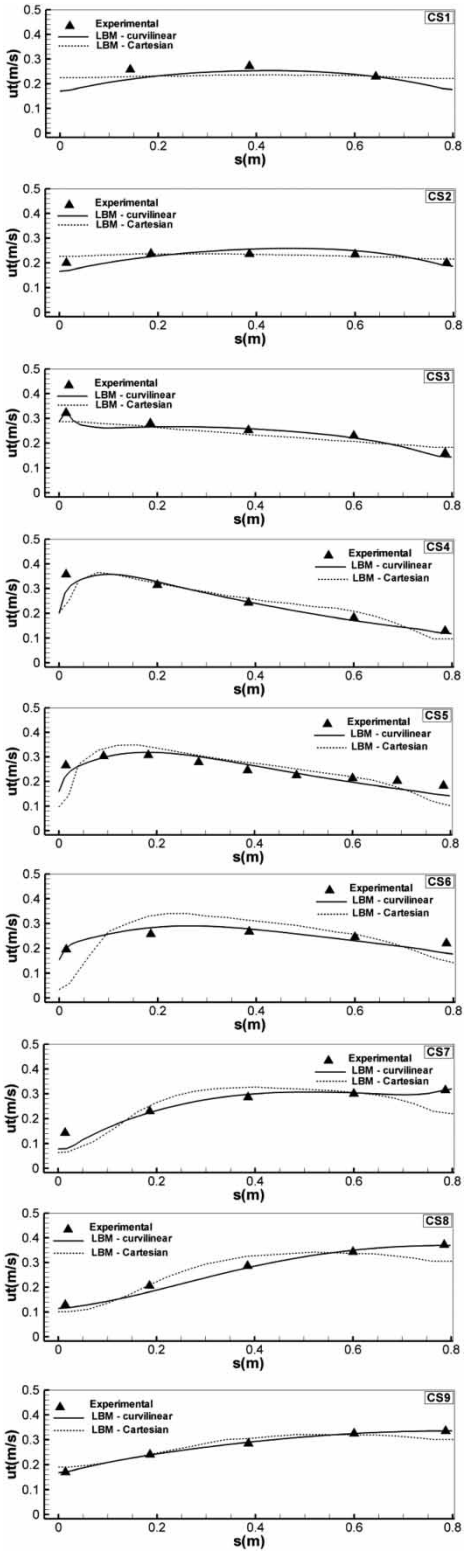

Figure 11 | Tangential velocities averaged along the vertical axis, comparison of measured and calculated values.

convex side of the flume in *CS4* and *CS7*, not exceeding 0.06 m s^{-1}. This is acceptable bearing in mind the extensively 3D character of the flow and the possible measurement errors. Moreover, calculated water levels given as contour lines in Figure 10 comply well with the measured values. As demonstrated, the physical rules characteristic to this type of flow are fully satisfied; the water level drops along the convex side of the bend due to the increased velocities, while the opposite is true along the concave side for the reduced velocities. The measured water levels are slightly higher than the calculated ones, which can be explained as combined influence of the significantly 3D character of the flow and measurement uncertainty.

CONCLUSIONS

Modeling flows in domains of complex geometry with the LBM, especially the application of the boundary conditions, is a demanding and complicated task. It sets an additional load on a computer, accompanied by deterioration of the solution in terms of accuracy. For that reason, a new form of LBM has been proposed here for overcoming these difficulties. Utilizing the method of complete transformation of the 2D flow equations from the physical in the computational domain, the resulting transformed equations were implemented in the rectangular LBM. Since the complete calculation is then performed in the basic, classical LBM environment, no further expressions and models are required for describing the boundary conditions and other elements usually associated with modeling complex physical domains. In the LBM domain, the most simple basic forms are used for describing the boundary conditions. Furthermore, the utilized computational procedures simulate a rather natural form of flow parameters (velocities), fitting better to the flow domain of interest. As a consequence, the accuracy of the resulting solution is improved in general, while the fundamental simplicity of the model is maintained. This has been demonstrated through three test examples. The results prove that the proposed form of the LBM stands for an efficient and high quality tool for solving cases of 2D flows with extremely complex 'natural' boundaries. This qualifies the method for extensive application.

REFERENCES

Bouzidi, M., d'Humières, D., Lallemand, P. & Luo, L. S. 2001 Lattice Boltzmann Equation on a two-dimensional rectangular grid. *J. Comput. Phys.* **172**, 704–717.

Chen, S., Martinez, D. & Mei, R. 1996 On boundary conditions in lattice Boltzmann methods. *Phys. Fluids* **8**, 2527–2536.

Cheng, M. & Hung, K. C. 2004 Lattice Boltzmann Method on nonuniform mesh. *Intl. J. Comput. Eng. Sci.* **5**, 291–302.

Dupuis, A. & Chopard, B. 2003 Theory and applications of an alternative lattice Boltzmann grid refinement algorithm. *Phys. Rev.* **E 67**, 066707-1–066707-7.

Filippova, O. & Hänel, D. 1998 Grid refinement for Lattice-BGK Models. *J. Comput. Phys.* **147**, 219–228.

Guo, Z. & Zhao, T. S. 2003 Explicit finite-difference lattice method for curvilinear coordinates. *Phys. Rev. E* **67**, 1–12.

Guo, Z., Zheng, C. & Shi, B. 2002 An extrapolation method for boundary conditions in lattice Boltzmann method. *Phys. Fluids* **14**, 2007–2010.

Han, S. L., Zhu, P. & Lin, Z. Q. 2007 Two-dimensional interpolation-supplemented and Taylor-series expansion-based lattice Boltzmann method and its application. *Commun. Nonlinear Sci. Numer. Simul.* **12**, 1162–1171.

He, X. & Doolen, G. 1997 Lattice Boltzmann method on curvilinear coordinates system: flow around a circular cylinder. *J. Comput. Phys.* **134**, 306–315.

He, X., Luo, L. S. & Dembo, M. 1996 Some progress in lattice Boltzmann method. Part I. Nonuniform mesh grids. *J. Comput. Phys.* **129**, 357–363.

Joshi, H., Agarwal, A., Puranik, B., Shu, C. & Agrawal, A. 2009 A hybrid FVM–LBM method for single and multi-fluid compressible flow problems. *Intl. J. Numer. Meth. Fluids* **62**, 403–427.

Kang, J., Kang, S. & Suh, Y. K. 2008 A dynamic boundary model for implementation of boundary conditions in lattice-Boltzmann method. *J. Mech. Sci. Tech.* **22**, 1192–1201.

Koelman, J. M. V. A. 1991 A simple lattice Boltzmann scheme for Navier-Stokes fluid flow. *Europhys. Lett.* **15**, 603.

Kranenburg, C. 1992 Wind-driven chaotic advection in a shallow model lake. *J. Hydraul. Res.* **30**, 29–46.

Lätt, J., Chopard, B., Malaspinas, O., Deville, M. & Michler, A. 2008 Straight velocity boundaries in the lattice method. *Phys. Rev.* **E 77**, 056703-1–056703-16.

Lee, J. & Lee, S. 2010 Boundary treatment for the lattice method using adaptive relaxation times. *Comp. Fluids* **39**, 900–909.

Li, Q., He, Y. L. & Gao, Y. J. 2008 Implementation of finite-difference lattice Boltzmann method on general body-fitted curvilinear coordinates. *Intl. J. Mod. Phys.* **19**, 1581–1595.

Lin, C. L. & Lai, Y. G. 2002 Lattice Boltzmann method on composite grids. *Phys. Rev. E* **62**, 2219–2225.

Liu, H., Zhou, J. G. & Burrows, R. 2009 Multi-block lattice Boltzmann simulations of subcritical flow in open channel junctions. *Comput. Fluids* **38**, 1108–1117.

Lu, Z., Liao, Y., Qian, D., McLaughlin, J. B., Derksen, J. J. & Kontomaris, K. 2002 Large Eddy simulations of a stirred tank using the lattice Boltzmann method on a nonuniform grid. *J. Comput. Phys.* **181**, 675–704.

McNamara, G. R. & Zanetti, G. 1988 Use of the Boltzmann equation to simulate lattice-gas automata. *Phys. Rev. Lett.* **61**, 2332–2335.

Mei, R. W. & Shyy, W. 1998 On the finite difference-based Boltzmann method in curvilinear coordinates. *J. Comput. Phys.* **143**, 426–448.

Mei, R. W., Luo, L. S. & Shyy, W. 1999 An accurate curved boundary treatment in the lattice Boltzmann method. *J. Comput. Phys.* **155**, 307–315.

Peng, G., Xi, H., Duncan, C. & Chou, S. H. 1998 Finite volume scheme for the lattice Boltzmann method on unstructured meshes. *Phys. Rev. E* **59**, 4675–4682.

Rivet, J. P. & Boon, J. P. 2001 *Lattice Gas Hydrodynamics*. Cambridge University Press, London, 298 pp.

Rothman, D. H. & Zaleski, S. 1997 *Lattice-gas Cellular Automata – Simple Models of Complex Hydrodynamics*. Cambridge University Press, London, 297 pp.

Rozovskii, I. L. 1963 *Flow of Water in Bends in Open Channels*. Academy of Sciences of the Ukrainian SSR, Israel Program for Scientific Translation in Kiev, Jerusalem.

Shu, C., Chew, Y. T. & Niu, X. D. 2001 Least-squares-based lattice Boltzmann method: a meshless approach for simulation of flows with complex geometry. *Phys. Rev. E* **64**, 045701-1–045701-4.

Shu, C., Niu, X. D. & Chew, Y. T. 2002 Taylor-series expansion and least-squares-based lattice Boltzmann method: two-dimensional formulation and its applications. *Phys. Rev. E* **65**, 036708-1–036708-13.

Simmonds, J. G. 1994 *A Brief on Tensor Analysis*. Springer, New York, 112 pp.

Stiebler, M., Tölke, J. & Krafczyk, M. 2006 An upwind discretization scheme for the finite volume lattice Boltzmann method. *Comput. Fluids* **35**, 814–819.

Ubertini, S., Bella, G. & Succi, S. 2003 Lattice Boltzmann method on unstructured grids: further developments. *Phys. Rev.* E **68**, 016701-1–016701-10.

Verschaeve, J. C. G. & Müller, B. 2010 A curved no-slip boundary condition for the lattice Boltzmann method. *J. Comput. Phys.* **229**, 6781–6803.

Yu, D., Mei, R. & Shyy, W. 2002 A multi-block lattice Boltzmann method for viscous fluid flows. *Intl. J. Numer. Meth. Fluids* **39**, 99–120.

Yu, D., Mei, R., Luo, L. S. & Shyy, W. 2003 Viscous flow computations with the method of lattice Boltzmann equation. *Progr. Aerospace Sci.* **39**, 329–367.

Zhou, J. G. 2004 *Lattice Boltzmann Methods for Shallow Water Flows*. Springer-Verlag, Berlin, 112 pp.

Zhou, J. G. 2010 Rectangular lattice Boltzmann method. *Phys. Rev. E* **81**, 026705-1–026705-10.

First received 21 July 2011; accepted in revised form 21 November 2011. Available online 9 March 2012